# Lamprophyre dikes of northern Idaho and northeastern Washington

Andrew M. Buddington
Cody J. Steven
Basil Tikoff
Richard M. Gaschnig

# Lamprophyre dikes of northern Idaho and northeastern Washington

Andrew M. Buddington [1]
Cody J. Steven [2]
Basil Tikoff [3]
Richard M. Gaschnig [4]

## ABSTRACT

Fifteen Paleogene lamprophyre dikes from northern Idaho and northeastern Washington were sampled for mineralogical and geochemical characterization. The lamprophyres occur as fine-grained narrow dikes and are undeformed. Kersantite and spessartite are the dominant rock types with lesser minette. Geochemically, the dikes are high-K calc-alkaline to shoshonitic, with $SiO_2$ contents ranging from 42.5 to 56.1 weight percent, and $K_2O$ from 2.3 to 6.7 weight percent. Ni and Cr contents are 28 to 215 ppm and 31 to 454 ppm, respectively, with Mg#s ranging from 52 to 73. Chondrite-normalized REE patterns are strongly fractionated with highly enriched LREE ($La_n$ = 98 to 692) to moderately enriched HREE ($Lu_n$ = 6 to 12). One sample from within the western Idaho shear zone (WISZ) is the least primitive lamprophyre (Mg# = 52) and exhibits an $^{40}Ar/^{39}Ar$ date of 46.77 ± 0.26 Ma. None of the other samples have been dated but are presumed to be post-middle Eocene due to their undeformed nature and proximity to the early Eocene Priest River complex, one of the many metamorphic core complexes occurring in Pacific Northwest. Geochemically (and geochronologically), these rocks correlate to potassic volcanic rocks of the Yellow Lake area (south-central British Columbia), along with lamprophyre dikes described from the margins of the Valhalla and Monashee complexes (southeast British Columbia), and mafic potassic rocks of the Montana alkaline province (Highwood Mountains).

## INTRODUCTION

Lamprophyres are melanocratic to mesocratic igneous rocks, commonly exhibiting a panidiomorphic texture with mafic phenocrysts of dark mica and/or amphibole (Wooly and others, 1996). Lamprophyres may or may not have pyroxene or olivine, and the feldspars (and feldspathoids) are typically restricted as groundmass phases. Lamprophyre intrusions commonly occur as hypabyssal dikes and sills but can form shallow stocks or plugs. Chemically, lamprophyres are subdivided into three groups: calc-alkaline, alkaline, and ultramafic lamprophyres; see Rock (1987) for specific chemical criteria. Calc-alkaline lamprophyres are weakly silica-saturated to undersaturated, are typically melanocratic, and are rich in dark mica and/or amphibole. Calc-alkaline lamprophyres are subdivided based on the dominant phenocryst versus groundmass (feldspar) phases with the four most common types being minette, kersantite, vogesite, and spessartite.

The lamprophyres described in this study are high-K calc-alkaline to shoshonitic series, with kersantite and spessartite being the dominant types. Minette, although present, occurs in fewer numbers. Although lamprophyric rocks have been recognized and mapped within the Coeur d'Alene mining district (Shannon, 1920; Hobbs and others, 1965), no detailed study of lamprophyric rocks from northern Idaho outside the district has been completed. The mafic potassic rocks described here are similar both mineralogically and geochemically to lamprophyric occurrences in

[1]Science Department, Spokane Community College, 1810 Greene St, Spokane, Washington, 99217 USA
[2]Department of Geography and Geological Sciences, University of Idaho, 875 Perimeter Dr, MS 3022, Moscow, Idaho 83844, USA
[3]Department of Geoscience, University of Wisconsin, 1215 W Dayton St, Madison, Wisconsin 53706, USA
[4]Department of Environmental, Earth, and Atmospheric Sciences, University of Massachusetts Lowell, 1 University Ave, Lowell, MA 01854, USA

other parts of the Inland Northwest and the northern Rocky Mountain region, most of which are associated with Eocene magmatism (O'Brien and others, 1991; Breitsprecher and others, 2003; Dostal and others, 2003; Sevigny and Thériault, 2003; Adams and others, 2005).

The source and setting of the Eocene lamprophyres remain debated. In their study of analcime-bearing, potassic volcanic rocks of the Challis-Kamloops belt of south-central British Columbia, Dostal and others (2003) propose melting of Precambrian lithospheric mantle within a slab window environment during the Eocene as the primary magmatic mechanism. Shoshonitic mafic dikes intruding the southern portion of the Monashee complex of southeastern British Columbia are described by Adams and others (2005). They suggest the dikes were generated by decompression melting of metasomatized lithospheric mantle and emplaced during Eocene extension. Sevigny and Thériault (2003) present major- and trace-element geochemistry along with Sm/Nd isotopic compositions of lamprophyric dikes along the edge of the Valhalla complex of southeastern British Columbia. They attribute the source of these dikes to decompression melting of an uncontaminated mantle reservoir during Eocene extension. O'Brien and others (1991, 1995) provide detailed geochemical and mineralogical data on various mafic potassic to ultrapotassic rocks (including minettes) from the Highwood Mountains of the Montana alkaline province. The Highwood magmas are attributed to a complex history of subduction (to post-subduction, slab rollback) generated partial melting (of enriched mantle asthenosphere), including mixing and degassing into shallow crustal levels during the Eocene.

The purpose of this study is to describe the mineralogy and major- and trace-element geochemistry of the dikes from northern Idaho, and to compare them with other well-studied lamprophyre (or mafic potassic) occurrences throughout southern British Columbia and western Montana.

## LOCATIONS

A total of fifteen lamprophyre dikes were sampled and described in this study (Figure 1). Numerous lamprophyric dikes (>25) have been mapped or described throughout the Coeur d'Alene mining district of northern Idaho (Shannon, 1920; Hobbs and others, 1965). However, because of the lack of detailed location data and the difficulty of access, only three of the Coeur d'Alene district dikes were sampled for this study. The fifteen dikes reported in this study were targeted based on location data obtained from Reed Lewis of the Idaho Geological Survey (see Appendix 1).

The majority of samples (11) occur directly east of the Purcell Trench fault, the eastern bounding fault of the Priest River complex (PRC), and intrude Mesoproterozoic metasedimentary rocks of the Belt Supergroup (Figure 1). Of these samples east of the Purcell Trench fault, three are from the Coeur d'Alene mining district. Two samples are from the western margin of the PRC; one intrudes the early Eocene Silver Point pluton, the second intrudes limestones of the upper Cambrian Metaline Formation. Two outcrops occur just west of the Clearwater complex where they intrude metamorphosed rocks of the Belt Supergroup. The last sample is from a dike that intrudes amphibolite-grade orthogneiss within the western Idaho shear zone (WISZ) along the main Salmon River, just east of Riggins, Idaho. The lamprophyre from the WISZ is located approximately 100 miles south of the Clearwater complex samples, and approximately 200 miles south of the Priest River complex samples.

## LITHOLOGY AND MINERALOGY

All samples were slabbed and stained to determine feldspar type and modal abundance, and then examined under a petrographic microscope to characterize textures and identify minerals. Mineral compositions were confirmed using Energy-dispersive X-ray spectroscopy. Twelve of the dikes sampled are melanocratic (color index values >60), with two dikes exhibiting a mesocratic color index (Figure 2). Calc-alkaline lamprophyre type classification (Rock, 1987; Winter, 2001) is based on the dominant phenocryst and groundmass feldspar assemblages:

- Minette: biotite/phlogopite>amphibole, K-feldspar>plagioclase

- Kersantite: biotite/phlogopite>amphibole, plagioclase>K-feldspar

- Vogesite: amphibole>biotite/phlogopite, K-feldspar>plagioclase

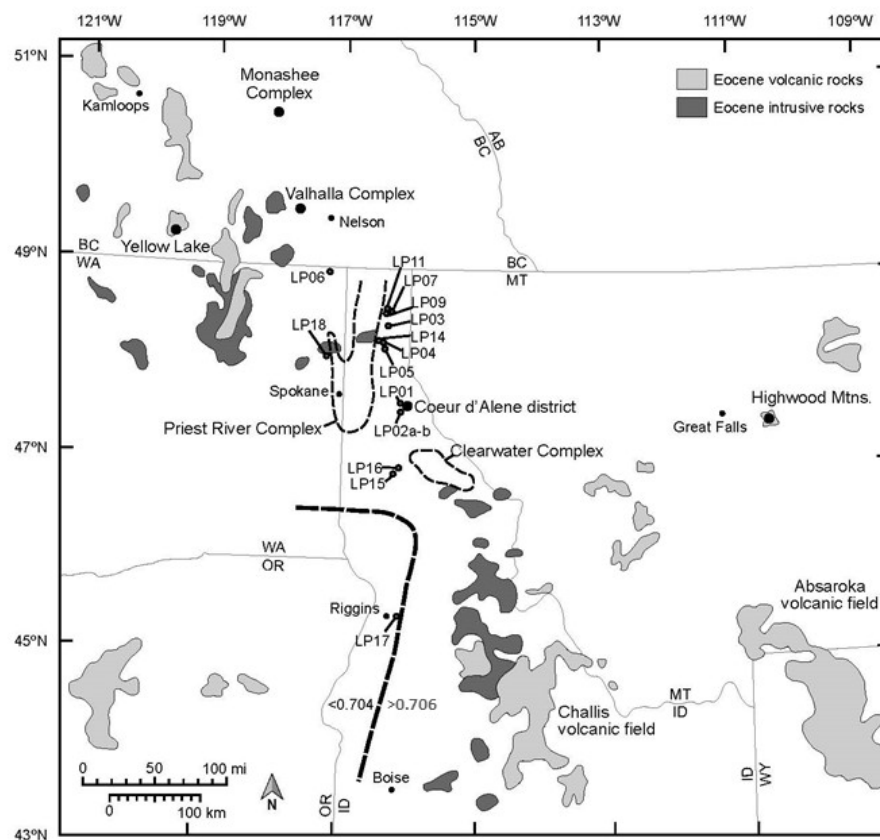- Spessartite: amphibole>biotite/phlogopite, plagioclase>K-feldspar

Figure 1. Regional location map. Locations and sample numbers (LP01 to LP18) of Eocene lamprophyre dikes (from this study) and other Eocene magmatic rocks of the Inland Northwest (modified from Lewis and others, 2020). The 0.704-0.706 initial $^{87}Sr/^{86}Sr$ line derived from Fleck and Criss (2007). The western Idaho shear zone (WISZ) is generally coincident with the 0.706 line. Note that sample LP17 is the Salmon River sample location.

In general, the dikes are not foliated and weakly to moderately porphyritic. Phenocryst minerals include phlogopite/biotite, hornblende, magnesiohornblende, and diopsidic augite (Figure 3). The dominant groundmass phases include plagioclase, potassium feldspar, biotite, clinopyroxene, hornblende, and apatite, with accessory Fe/Ti oxides, titanite, olivine, carbonate, rutile, pyrite, and rare feldspathoid. In thin section, the rocks commonly exhibit panidiomorphic textures with biotite, hornblende, and rare clinopyroxene as phenocrysts. The phenocrysts are generally euhedral with variable degrees of fracturing. Biotite phenocrysts commonly have dark brown rims (Fe and Ti rich) and pale, phlogopitic cores (Figure 3c). In the minettes and kersantites, biotite may exhibit castellated form (Figure 3a, 3c). Castellated (battlemented) form typifies biotites

(and phlogopites) within lamprophyres. This texture appears to be exclusively associated with lamprophyric rocks and has no known explanation for a process of formation (Rock and others, 1991). In the spessartites, hornblende, magnesiohornblende, and diopsidic augite are euhedral to subhedral, show variable fracturing, resorption, and rare sieve-like textures (Figure 3f). Olivine was identified in one sample (LP06) where it occurred in cumulophyric clots with clinopyroxene and biotite (Figure 3k). Groundmass feldspars are typically very fine grained, and lath or needle shaped.

The lamprophyres of this study generally exhibit minor to moderate alteration. A few samples exhibit advanced alteration of phenocrysts, where talc and spinel replaced olivine. (Fig. 3g, 3l). Another phenocryst alteration is relatively minor with chlorite after clinopyroxene and
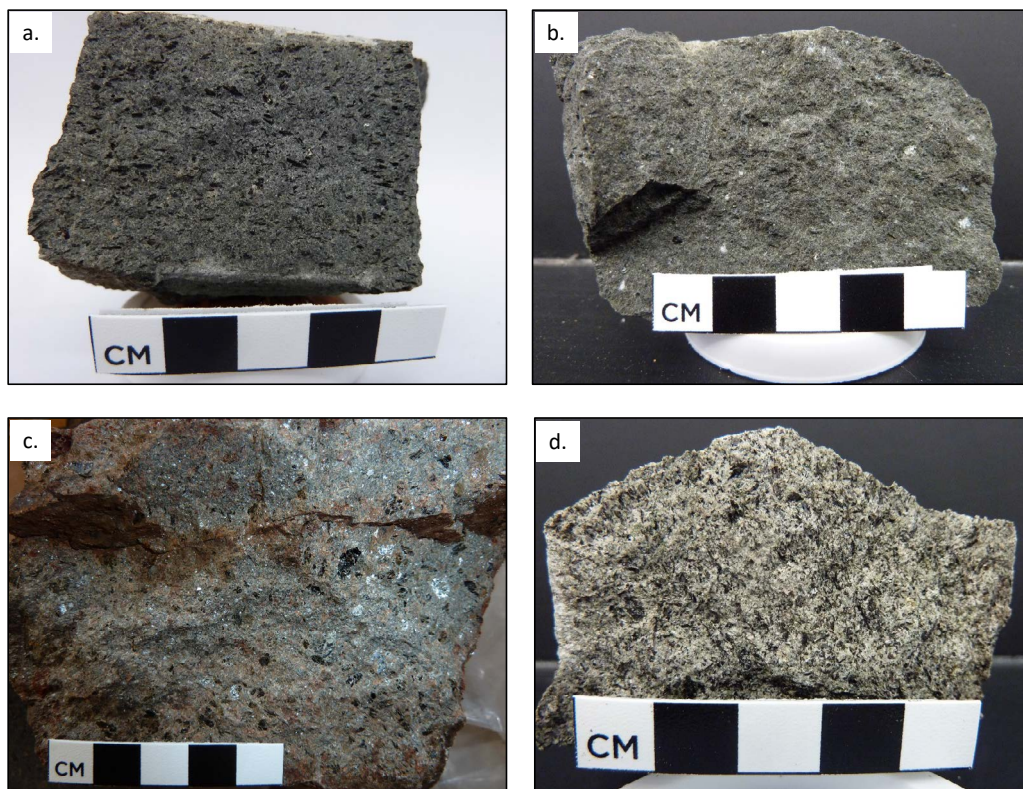
Figure 2.  Lamprophyre hand samples from this study. (a) phlogopite-clinopyroxene kersantite (LP02); (b) phlogopite-gedrite spessartite (LP01); (c) phlogopite-clinopyroxene minette (LP04); (d) hornblende-phlogopite spessartite (LP05).

amphibole. Biotite phenocrysts typically exhibit Fe-rich rims with minimal alteration. Other alteration phases include sericite, clay, epidote, and quartz. Alteration of groundmass phases is more prominent with feldspars (plagioclase shows greater alteration than K-feldspar) variably altered to carbonate, sericite, and/or epidote. Rare serpentine occurs in the groundmass of some samples. Opaque minerals are dominated by groundmass magnetite and lesser ilmenite, with titanite and Cr-spinel occurring in accessory amounts.

Ocelli and light-colored globular structures (ranging from 1 to 3 cm) are relatively rare in the dikes sampled for this study. One sample (LP18), which intrudes the Silver Point pluton on the northwest side of the Priest River complex, contains abundant light-colored globules (ocelli), along with xenoliths of granitic country rock. Rare xenocrystic quartz was observed in thin section (Figure 3l). Three basic types of ocelli or globular structures are described by Rock and others (1991): (i) carbonate-analcime, (ii) feldspathic (syenitic +/- feldspathoids), and (iii) carbonate-chlorite/serpentine-epidote-quartz+/-feldspar+/-zeolites. Although the ocelli observed in this study were not studied in petrographic detail, Rock and others (1991) report that types ii and iii can be associated with calc-alkaline lamprophyres. Philpots (1976) and Eby (1980) suggest lamprophyric ocelli are the result of magmatic crystallization of two immiscible liquids, while Cooper (1979) argues for the segregation of late-stage magmatic liquids for ocellar lamprophyres from New Zealand.

# MAJOR- AND TRACE-ELEMENT ANALYSES

The dike samples were split and cleaned of weathered surfaces and any xenoliths or light-colored globules (ocelli). The samples were analyzed by X-ray fluorescence (XRF) and inductively coupled plasma mass spectrometry (ICP-MS) at the Washington State University GeoAnalytical Laboratory (Table 1).
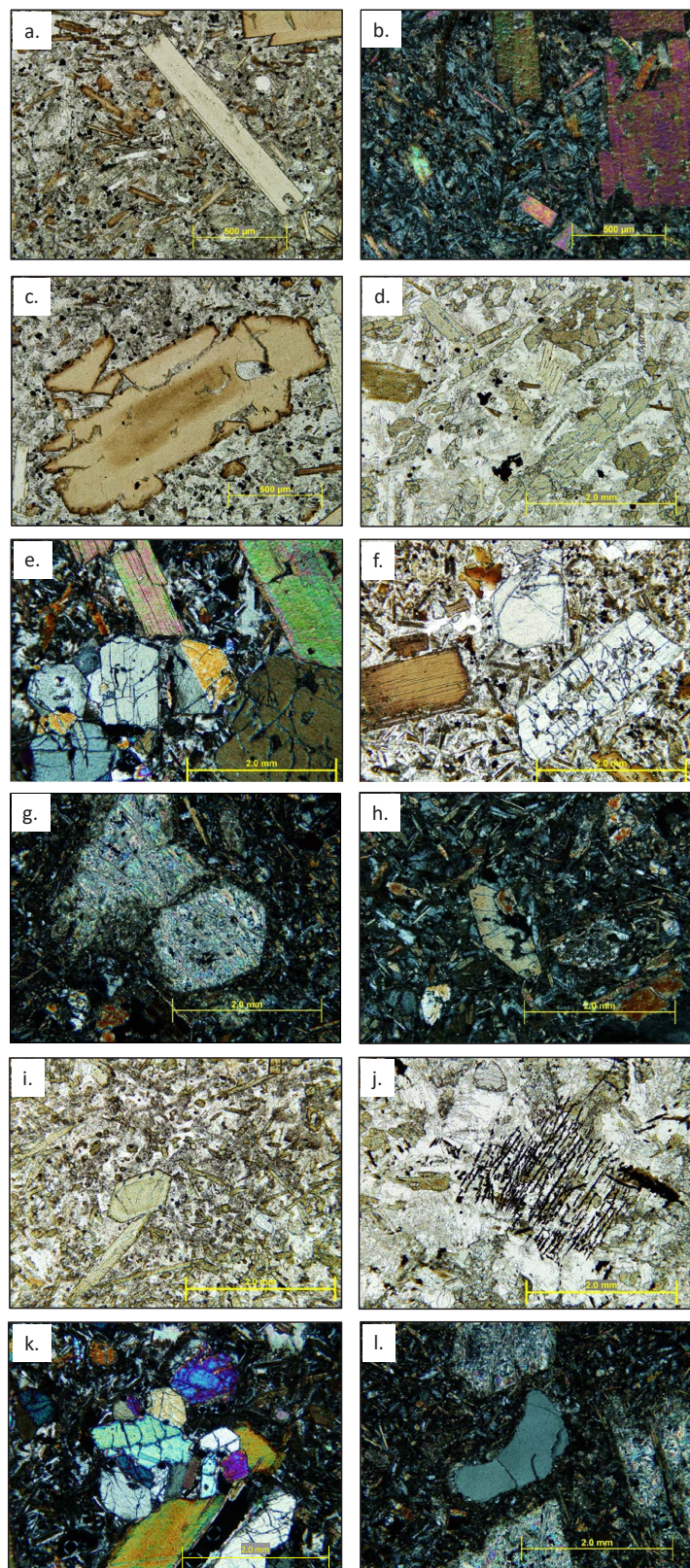
4

Figure 3. Photomicrographs of lamprophyre minerals and textures. (a) panidiomorphic texture with partially castellated phlogopitic mica and accessory apatite in plane polarized light (PPL), (LP02); (b) phlogopitic mica and feathery feldspathoid in matrix in cross polarized light (XPL), (LP02); (c) zoned phlogopitic mica with Fe-enriched rims (PPL), (LP02); (d) broken amphibole (green-brown) with phlogopitic mica in altered matrix (PPL), (LP05); (e) diopsidic augite with phlogopitic mica (XPL), (LP06); (f) sieve-textured diopsidic augite with biotite (PPL), (LP06); (g) talc and spinel after pyroxene (XPL), (LP01); (h) partially resorbed magnesiohornblende with matrix of amphibole and plagioclase (XPL), (LP01); (i) zoned hornblende phenocryst and micro-phenocrysts with phlogopite and epidote (PPL), (LP07); (j) skeletal ilmenite with clinopyroxene, hornblende, accessory titanite, and chlorite/carbonate alteration (PPL), (LP16); (k) glomerocryst of diopsidic augite with biotite and olivine (XPL), (LP06); (l) xenocrystic quartz with altered pyroxene phenocrysts and matrix (XPL), (LP01).

Table 1. Major- and trace-element geochemistry of lamprophyre samples from northern Idaho and northeastern Washington.

| Sample number | LP01 | LP02A | LP02B | LP03 | LP04 | LP05 | LP06 | LP07 | LP09 | LP11 | LP14 | LP15 | LP16 | LP17 | LP18 |
|---|---|---|---|---|---|---|---|---|---|---|---|---|---|---|---|
| $SiO_2$ (wt.%) | 47.46 | 49.11 | 56.09 | 54.56 | 52.10 | 51.08 | 50.14 | 51.21 | 54.64 | 53.98 | 50.69 | 55.28 | 50.14 | 42.54 | 54.42 |
| $TiO_2$ | 1.23 | 1.26 | 0.84 | 0.91 | 0.82 | 1.71 | 0.89 | 0.85 | 1.10 | 0.99 | 1.42 | 1.55 | 2.06 | 4.31 | 0.94 |
| $Al_2O_3$ | 12.74 | 13.82 | 14.76 | 13.51 | 12.48 | 12.05 | 14.92 | 14.73 | 12.97 | 13.15 | 12.53 | 16.25 | 14.65 | 13.48 | 13.03 |
| $FeO_t$ | 8.92 | 6.73 | 6.04 | 5.15 | 7.03 | 7.83 | 6.79 | 6.80 | 7.66 | 7.31 | 5.26 | 6.89 | 8.88 | 11.07 | 5.67 |
| MnO | 0.16 | 0.11 | 0.10 | 0.10 | 0.13 | 0.12 | 0.10 | 0.12 | 0.14 | 0.12 | 0.12 | 0.11 | 0.13 | 0.20 | 0.10 |
| MgO | 9.59 | 5.67 | 7.55 | 4.65 | 6.63 | 7.13 | 5.27 | 8.82 | 6.78 | 8.40 | 4.06 | 4.24 | 7.50 | 6.02 | 6.82 |
| CaO | 8.53 | 7.25 | 5.36 | 5.69 | 5.92 | 8.29 | 6.42 | 6.94 | 6.61 | 6.58 | 7.73 | 4.49 | 6.86 | 10.90 | 6.08 |
| $Na_2O$ | 1.87 | 1.86 | 3.15 | 2.70 | 1.90 | 2.72 | 1.88 | 3.17 | 3.00 | 2.69 | 1.73 | 3.80 | 3.16 | 1.94 | 3.09 |
| $K_2O$ | 2.37 | 6.13 | 2.34 | 5.07 | 5.05 | 5.30 | 3.94 | 2.78 | 3.29 | 3.40 | 6.72 | 2.64 | 2.14 | 3.16 | 5.68 |
| $P_2O_5$ | 0.55 | 1.18 | 0.28 | 1.23 | 0.67 | 1.77 | 0.53 | 0.63 | 0.51 | 0.55 | 1.46 | 0.40 | 0.41 | 1.16 | 1.57 |
| LOI % | 5.29 | 5.70 | 2.49 | 4.96 | 6.18 | 0.81 | 8.37 | 2.69 | 2.40 | 2.03 | 6.10 | 3.24 | 3.27 | 4.44 | 0.75 |
| Total | 98.70 | 98.83 | 98.99 | 98.52 | 98.90 | 98.81 | 99.25 | 98.74 | 99.11 | 99.20 | 97.82 | 98.88 | 99.22 | 99.21 | 98.14 |
| | | | | | | | | | | | | | | | |
| Ni* (ppm) | 180 | 155 | 195 | 73 | 144 | 152 | 28 | 215 | 84 | 204 | 64 | 93 | 195 | 41 | 184 |
| Cr* | 433 | 208 | 334 | 149 | 245 | 248 | 122 | 454 | 345 | 436 | 111 | 98 | 278 | 31 | 283 |
| V* | 200 | 145 | 126 | 111 | 151 | 166 | 144 | 144 | 183 | 154 | 112 | 131 | 169 | 326 | 102 |
| Ga* | 17 | 18 | 20 | 16 | 17 | 19 | 18 | 19 | 19 | 18 | 19 | 19 | 19 | 23 | 19 |
| Cu* | 43 | 47 | 23 | 39 | 52 | 43 | 24 | 24 | 51 | 42 | 41 | 52 | 27 | 80 | 87 |
| Zn* | 90 | 104 | 68 | 89 | 77 | 161 | 71 | 87 | 95 | 84 | 182 | 89 | 98 | 122 | 68 |
| La | 62.52 | 45.88 | 45.30 | 128.29 | 34.85 | 183.75 | 33.63 | 96.11 | 38.73 | 52.53 | 214.70 | 47.95 | 30.23 | 81.84 | 168.46 |
| Ce | 128.77 | 99.32 | 90.44 | 243.24 | 73.92 | 395.17 | 67.71 | 161.76 | 78.63 | 100.57 | 436.00 | 85.77 | 62.22 | 175.09 | 299.41 |
| Pr | 16.14 | 13.02 | 10.81 | 27.99 | 9.61 | 47.23 | 8.34 | 17.56 | 9.73 | 11.74 | 49.28 | 10.66 | 7.68 | 21.68 | 32.71 |
| Nd | 63.95 | 53.14 | 40.70 | 99.24 | 39.76 | 180.68 | 33.42 | 61.41 | 38.60 | 44.87 | 181.51 | 40.80 | 30.83 | 85.40 | 113.81 |
| Sm | 12.23 | 10.37 | 7.29 | 14.06 | 8.16 | 31.03 | 6.80 | 9.35 | 7.68 | 8.09 | 25.26 | 7.42 | 6.40 | 16.30 | 15.94 |
| Eu | 3.08 | 2.77 | 1.81 | 3.40 | 2.10 | 7.33 | 2.07 | 2.39 | 2.05 | 2.20 | 6.46 | 2.39 | 2.14 | 4.86 | 4.08 |
| Gd | 8.91 | 7.74 | 5.17 | 7.82 | 6.04 | 19.92 | 5.34 | 6.16 | 6.00 | 6.11 | 12.65 | 6.14 | 5.42 | 12.71 | 9.11 |
| Tb | 1.21 | 1.00 | 0.73 | 0.92 | 0.81 | 2.29 | 0.74 | 0.81 | 0.84 | 0.83 | 1.31 | 0.86 | 0.79 | 1.76 | 1.03 |
| Dy | 6.30 | 5.07 | 4.07 | 4.34 | 4.37 | 10.22 | 3.92 | 4.20 | 4.52 | 4.28 | 5.39 | 4.58 | 4.27 | 9.07 | 4.73 |
| Ho | 1.13 | 0.88 | 0.78 | 0.75 | 0.82 | 1.56 | 0.70 | 0.76 | 0.84 | 0.78 | 0.81 | 0.83 | 0.76 | 1.53 | 0.74 |
| Er | 2.90 | 2.17 | 2.03 | 1.86 | 2.02 | 3.31 | 1.78 | 1.94 | 2.10 | 1.93 | 1.73 | 2.06 | 1.81 | 3.61 | 1.78 |
| Tm | 0.39 | 0.28 | 0.29 | 0.24 | 0.28 | 0.40 | 0.24 | 0.26 | 0.29 | 0.26 | 0.20 | 0.26 | 0.24 | 0.46 | 0.22 |
| Yb | 2.35 | 1.73 | 1.80 | 1.53 | 1.74 | 2.19 | 1.51 | 1.61 | 1.77 | 1.63 | 1.19 | 1.54 | 1.40 | 2.57 | 1.36 |
| Lu | 0.35 | 0.26 | 0.28 | 0.24 | 0.24 | 0.28 | 0.24 | 0.24 | 0.27 | 0.23 | 0.16 | 0.23 | 0.20 | 0.37 | 0.19 |
| Ba | 1855 | 2399 | 1002 | 5866 | 1845 | 3221 | 1529 | 2010 | 1394 | 1746 | 9395 | 1419 | 877 | 617 | 5542 |
| Th | 10.05 | 9.85 | 7.32 | 16.40 | 10.32 | 23.76 | 8.11 | 13.99 | 7.55 | 7.68 | 19.88 | 5.78 | 3.55 | 8.53 | 31.24 |
| Nb | 10.51 | 15.73 | 8.45 | 73.74 | 9.37 | 23.76 | 15.87 | 26.09 | 9.25 | 13.77 | 69.69 | 17.61 | 20.69 | 90.38 | 44.91 |
| Y | 28.66 | 22.71 | 19.74 | 19.56 | 20.53 | 39.05 | 17.48 | 19.51 | 20.93 | 19.54 | 20.38 | 23.52 | 18.52 | 37.45 | 19.23 |
| Hf | 5.28 | 8.36 | 4.86 | 7.21 | 4.45 | 11.26 | 3.31 | 4.81 | 4.55 | 4.63 | 10.01 | 5.75 | 4.72 | 10.88 | 14.94 |
| Ta | 0.59 | 0.81 | 0.49 | 3.90 | 0.60 | 1.22 | 0.83 | 1.00 | 0.53 | 0.65 | 3.09 | 1.09 | 1.31 | 5.84 | 2.37 |
| U | 2.09 | 2.91 | 1.62 | 5.04 | 3.60 | 5.07 | 2.45 | 3.35 | 1.79 | 1.83 | 3.76 | 1.46 | 0.91 | 2.69 | 6.97 |
| Pb | 14.59 | 24.13 | 8.89 | 71.09 | 20.82 | 10.51 | 16.47 | 14.15 | 11.16 | 9.93 | 63.29 | 13.83 | 10.02 | 6.24 | 23.89 |
| Rb | 44.8 | 232.0 | 49.1 | 87.9 | 164.1 | 105.4 | 117.2 | 53.5 | 73.4 | 76.9 | 84.7 | 63.1 | 48.5 | 78.2 | 91.1 |
| Cs | 7.12 | 3.26 | 1.85 | 1.27 | 5.92 | 0.88 | 6.23 | 0.85 | 1.50 | 1.65 | 5.27 | 1.14 | 1.32 | 2.58 | 1.84 |
| Sr | 998 | 1077 | 828 | 1080 | 876 | 872 | 321 | 1491 | 854 | 1050 | 3532 | 654 | 673 | 1276 | 2681 |
| Sc | 25.4 | 17.3 | 16.0 | 14.1 | 19.2 | 19.2 | 16.9 | 18.2 | 21.5 | 19.5 | 12.2 | 12.7 | 18.2 | 22.3 | 14.6 |
| Zr | 211 | 330 | 189 | 293 | 174 | 433 | 129 | 198 | 178 | 185 | 405 | 254 | 200 | 493 | 607 |

All analysis performed at Washinngton State University GeoAnalytical Laboratory, Pullman, Washington.
Total Fe expressed as $FeO_t$. Rare earth elements and trace elements are by ICP-MS except for those with asterisk, which are by XRF.
LOI, Loss on ingition.

The SiO$_2$ content of the dikes ranges between 42.5 and 56.1 weight percent (%), although all but two samples are between 47.5 and 55.3% (Table 1). The one sample with the lowest SiO$_2$ (42.5%) is from the Salmon River area and occurs within the WISZ. This sample is anomalous in almost all the major and trace element binary plots compared to the dikes to the north. The lamprophyres have K$_2$O plus Na$_2$O contents of 4 to 9%, with most samples >5%. The overall K$_2$O contents range from 2.1 to 6.7%, and from the plot of total SiO$_2$ vs. K$_2$O, the samples range from high-K calc-alkaline to shoshonite series (Figure 4). The dikes have Al$_2$O$_3$ contents ranging between 12 and 17% with TiO$_2$ contents 0.7 to 2.0%. Note the Salmon River dike has the highest TiO$_2$, FeO$_t$, and CaO values. The dikes have MgO contents of 4 to 9% with Mg#s ranging from 52 to 73 (molar Mg/(Mg+0.85Fe) x 100). The majority of the dikes have Mg# values between 60 and 70; once again, the Salmon River sample has the lowest Mg# of 52. Loss on ignition (LOI) values range from 0.8 to 6.2%.

The compatible trace elements Ni and Cr range from 28 to 215 ppm and 98 to 454 ppm, respectively (Figure 5). The Salmon River sample once again is unusual when compared to the group as a whole, having the lowest Cr content of 31 ppm. The dikes show variation of abundances of Ba (617 to 9395 ppm) and Sr (321 to 3532 ppm), with one sample (LP14) having the highest values in both Ba and Sr.

The mantle-normalized trace element plot shows significant enrichment in large ion lithophile elements (LILE) relative to the high field strength elements (HFSE) (Figure 6). Ba and Th are approximately 100 to 1000 times primitive mantle values. Nb, Ta, P, Zr, and Ti exhibit distinctive negative anomalies. The only exception to this pattern is the Salmon River sample, which exhibits moderate enrichment in LILE (relative to HFSE), and has no negative Nb, Ta, or Ti anomalies. The trace element patterns of the northern Idaho lamprophyric rocks are similar to the Eocene mafic potassic rocks from the Yellow Lake area (Dostal
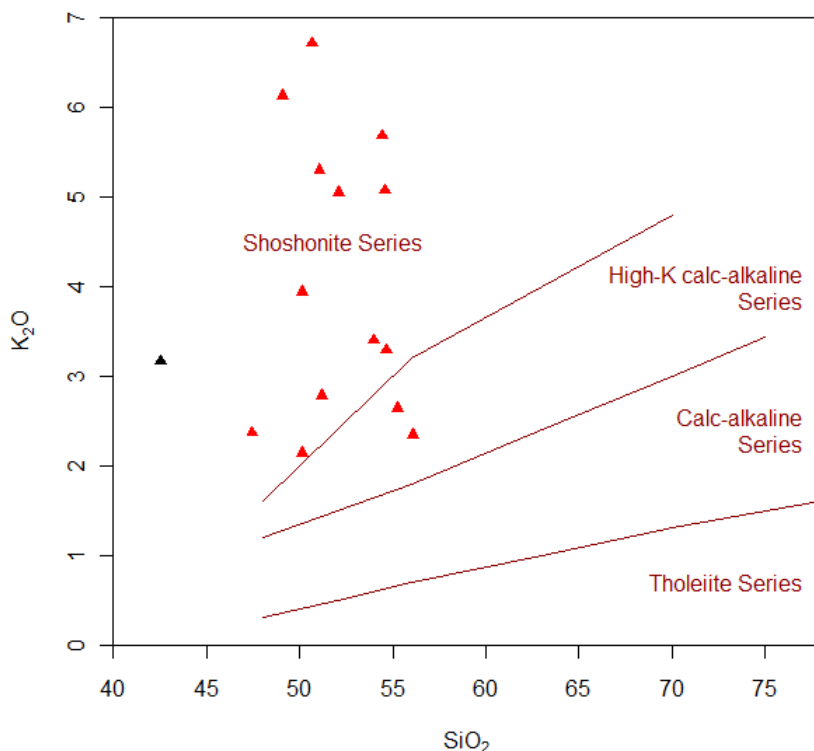


Figure 4.  SiO$_2$ vs. K$_2$O plot (after Pecerrillo and Taylor, 1976) showing lamprophyres of this study. The black triangle is the Salmon River sample (LP17) of this study.
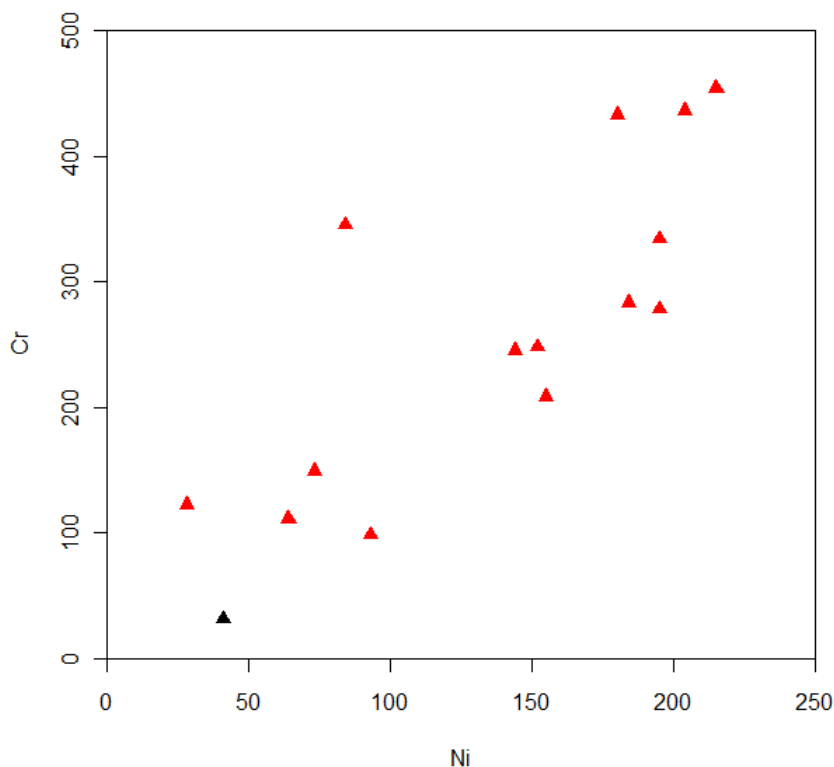
Figure 5.  Ni vs. Cr (ppm) plot for lamprophyres of this study. The black triangle is the Salmon River lamprophyre (LP17).

and others, 2003), the Monashee complex (Adams and others, 2005), the Valhalla complex (Sevigny and Theriault, 2003), and the Highwood Mountains of the Montana alkaline province (O'Brien and others, 1991; O'Brien and others, 1995).

The chondrite-normalized REE patterns for the northern Idaho lamprophyric rocks are steeply dipping from the light rare earth elements (LREE) to the heavy rare earth elements (HREE) with $La_n$ values between 100 to 700 (Figure 7) and $(La/Yb)_n$ ratios ranging from 14 to 121 (Table 2). All of the samples lack negative Eu anomalies. The REE abundances and patterns of the north Idaho lamprophyric rocks closely resemble those of other mafic potassic rocks from south-central British Columbia and the Highwood Mountains of the Montana alkaline province.

# AGES

A single lamprophyre from the Star Mine (Coeur d'Alene Mining District) was dated previously (K-Ar)

and yielded two ages with biotite at 50.7 ± 3.0 Ma and hornblende at 57.0 ± 1.5 Ma (McDowell, 1971). One age determination was made on the lamprophyres of this study. An $^{40}Ar/^{39}Ar$ biotite age of 46.77 ± 0.26 Ma (Figure 8) is from the lamprophyre dike (LP17) intruding the WISZ along the main Salmon River of west-central Idaho (see Appendix 2). This dike intrudes complexly deformed amphibolite-grade gneisses of the WISZ (Blake and others, 2009) and is undeformed, showing no metamorphic texture or fabric. Consequently, the lamprophyre dike crosscuts and postdates the ~100 to 90 Ma WISZ, consistent with timing estimates from other studies (Giorgis and others, 2008; Braudy and others, 2017).

We assume post middle Eocene ages for all the other dikes because they do not exhibit any deformational textures or fabrics. Further, all but one of the dikes occur in the hanging walls of the Priest River and Clearwater complexes, both of which experienced exhumation in early to middle Eocene time (Doughty and Price, 1999; Doughty and others, 2007). One of the dikes of this study (LP18) intrudes the foliated and variably
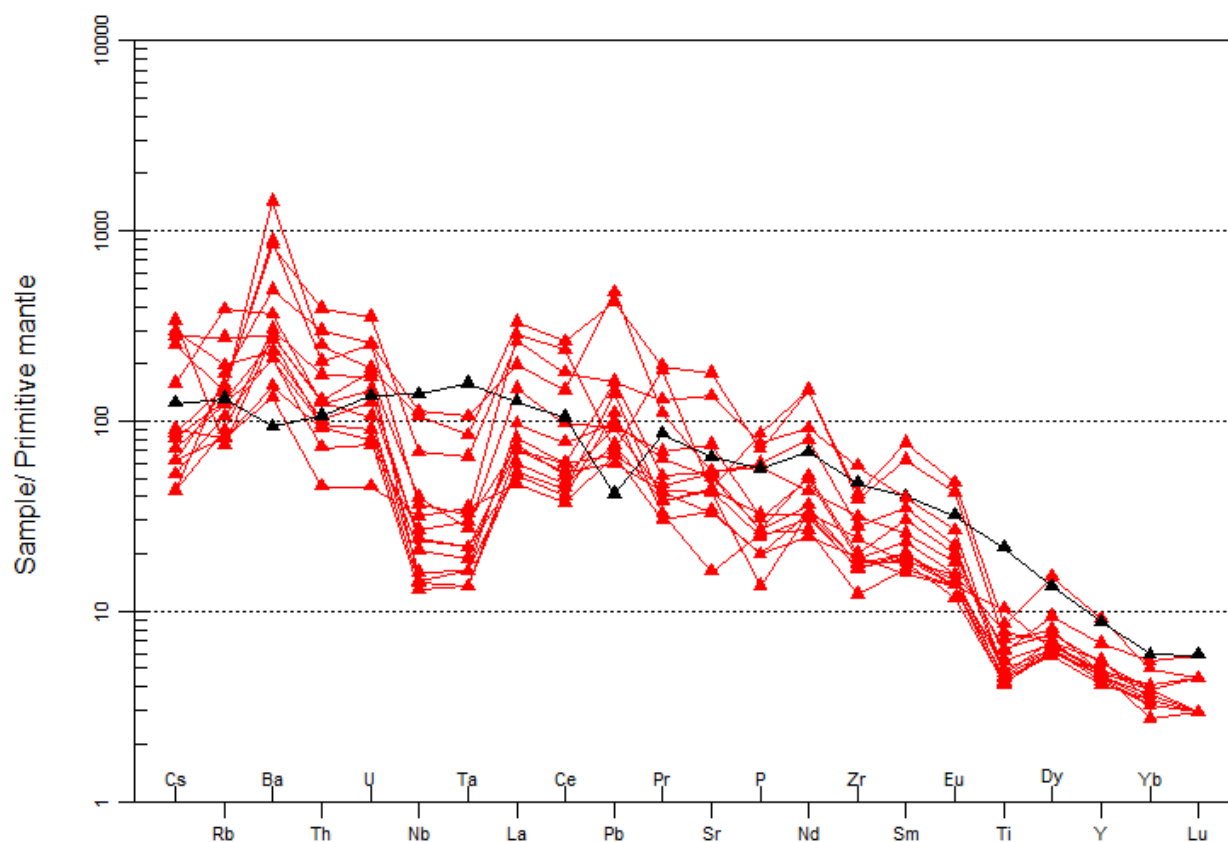
Figure 6. Primitive mantle normalized trace element plot for lamprophyres of this study (normalization from McDonough and Sun, 1995). The black triangles are the Salmon River lamprophyre (LP17).

mylonitized early Eocene Silver Point pluton along the eastern detachment of the Priest River complex.

# DISCUSSION

The lamprophyre dikes from northern Idaho and northeastern Washington bear many chemical similarities to mafic potassic igneous rocks of south-central British Columbia and the Highwood Mountains of the Montana alkaline province (Figure 9, Table 2). However, the alkali ratios from the dikes of this study exhibit greater variability when compared to other provinces (Figure 9). This may be in part due to the significantly broader area of sampling for this study possibly suggesting a more heterogeneous mantle source underlying northern Idaho. The lamprophyres of this study exhibit enriched (chondrite normalized) REE values with LILE enrichment vs. HFSE depletion

patterns, showing distinctive negative anomalies in Nb and Ta, and smaller negative troughs in Ti, P, and Zr. The rocks also exhibit significant positive anomalies in Ba and Pb. Although similarly enriched in trace elements, the one sample that does not exhibit the distinctive (negative or positive) anomalies is the Salmon River sample (Figure 6). Nonetheless, this distinctive decoupled pattern is typical of subduction zone generated magmas. This subduction signature could be associated with Paleogene subduction in the Pacific Northwest or represent a subduction signature inherited from previously metasomatized lithospheric mantle.

Calc-alkaline lamprophyres are typically associated with calc-alkaline granitoids of subduction environments. They can also, however, be associated alkaline-shoshonitic compositions inboard of a subduction-generated volcanic front (Rock, 1984; Winter, 2001). In the Highwood Mountains of the Montana
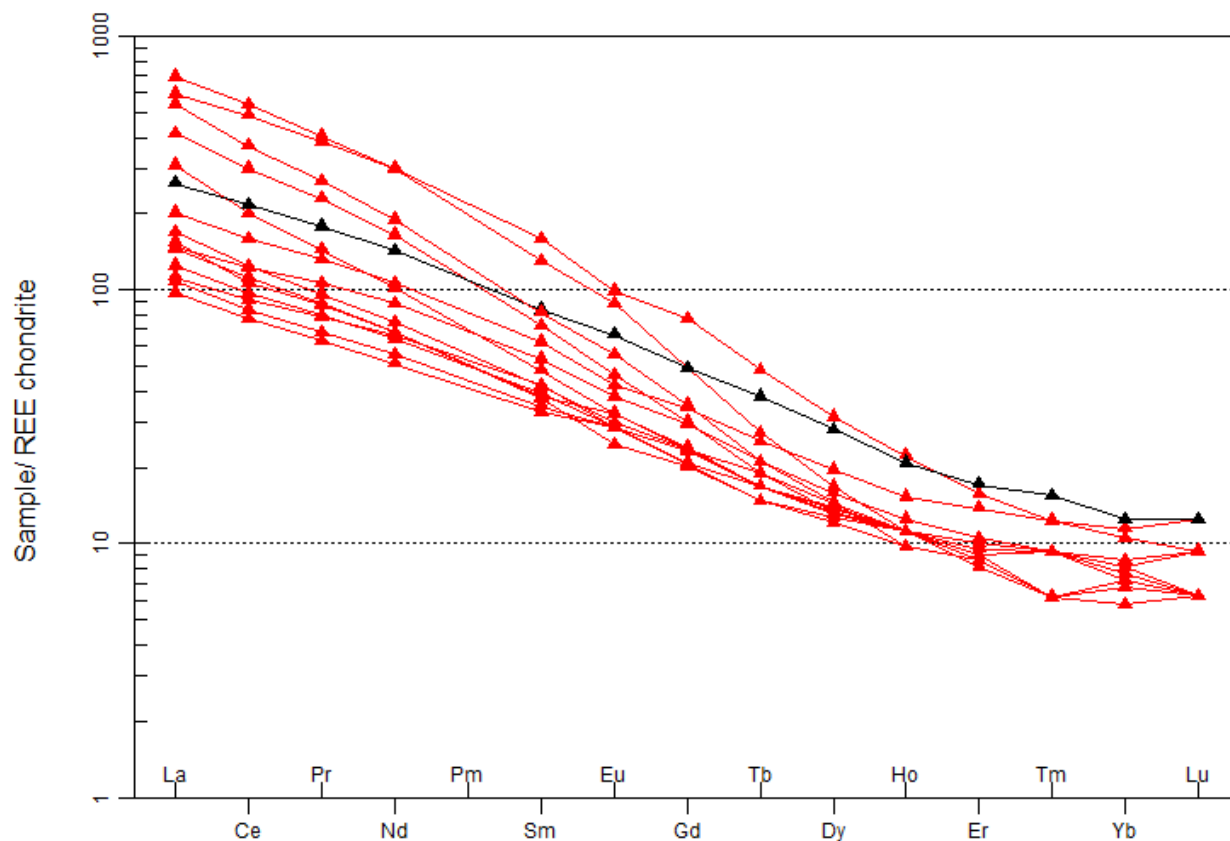
Figure 7. Chondrite normalized REE abundances for lamprophyres of this study (normalization from Boynton, 1984). The black triangles are the Salmon River lamprophyre (LP17).

alkaline province, lamprophyres and other potassic to ultrapotassic mafic rocks occur in a cogenetic suite of Eocene magmatism yet show similar subduction-related geochemical characteristics (O'Brien and others, 1991).

The Eocene-aged Salmon River sample (LP17) is clearly different from the other lamprophyres sampled in this study. It occurs significantly south of the main sample group and west of the Idaho batholith and established North American continental rocks. It occurs as a dike within an amphibolite-grade orthogneiss of the WISZ. Although it has the lowest overall SiO$_2$, it exhibits the least primitive composition (Mg# of 52) with the lowest Ni and Cr values. This sample overlaps and follows the same general REE and trace element patterns yet it exhibits none of the distinctive negative trace element anomalies of the other samples. The Salmon River sample is less enriched in normalized LILEs compared to the other lamprophyres and it has the lowest Ba value, with a weakly negative Ba anomaly (Figure 6).

It also lacks the characteristic negative Nb, Ta, P, Zr or Ti anomalies that all the other lamprophyre samples exhibit. The Salmon River sample has a pronounced negative anomaly in Pb whereas all the other samples show moderate to strongly positive Pb anomalies. And finally, the Salmon River sample is less enriched in LREE (relative to HREE) and has the highest HREE values of all the lamprophyre samples (Figure 7). Although no trace element modelling has been done, it appears difficult to explain these many differences by fractionation of a common parent magma. All of these differences suggest a different mantle source component for the Salmon River lamprophyre when compared to the northern Idaho and northeast Washington lamprophyres. LP17 intrudes the WISZ, which separates North American Precambrian crust to the east from the Blue Mountains province crust to the west. The Wallowa-Seven Devils terranes to the west are of well-documented island arc and oceanic affinity (Schmidt and others, 2016), and thus are distinct from

Table 2.  Selected major- (weight percent) and trace-element (ppm) values for various lamprophyric rocks from the Inland Northwest and British Columbia, Canada.

| | Valhalla | Monashee | Yellow Lk. | Highwoods | N. Idaho | Salmon River LP17 |
|---|---|---|---|---|---|---|
| | (n = 8) | (n = 9) | (n = 15) | (n = 3) | (n = 14) | (n = 1) |
| $SiO_2$% | 44.37 − 51.60 | 44.40 − 48.70 | 47.95 − 53.55 | 41.07-49.54 | 47.46 − 56.09 | 42.54 |
| $K_2O$% | 1.26 − 3.50 | 1.38 − 3.75 | 4.47 − 6.25 | 1.22 − 8.17 | 2.14 − 6.72 | 3.16 |
| MgO% | 5.01 − 9.46 | 5.85 − 9.21 | 1.49 − 4.75 | 4.49 − 18.07 | 4.06 − 9.59 | 6.02 |
| Ni | 28 − 204 | 42 − 190 | 7 − 73 | 24 - 533 | 28 - 215 | 41 |
| Mg# | 56 - 68 | 50 - 69 | - | - | 55 - 73 | 52 |
| Rb/Zr | 0.2 − 0.6 | 0.2 − 0.5 | 0.1 − 0.4 | 0.2 − 1.4 | 0.2 − 0.9 | 0.2 |
| $La_n/Yb_n$ | - | 9 − 51 | 63 − 88 | 17 − 60* | 14 - 121 | 22 |
| $Yb_n$ | 8.4 − 12.7 | 9 − 12 | 7 − 10 | 6 − 9* | 6 - 12 | 12 |
| Ba/Nb | 21 − 103 | 15 − 148 | 32 − 62 | 164 − 289 | 42 - 196 | 7 |
| Ba/Nb (avg) | 35 | 106 | 39 | 237 | 121 | - |

*values estimated from elemental plots.
Mg# = Mg/(Mg + .85Fe) x 100.
Data: Sevigny & Theriault, 2003 (Valhalla), Adams and others, 2005 (Monashee), Dostal and others, 2003 (Yellow Lk.), O'Brien and others, 1991 (Highwood Mountains minette samples only). N. Idaho, Salmon River = this study.
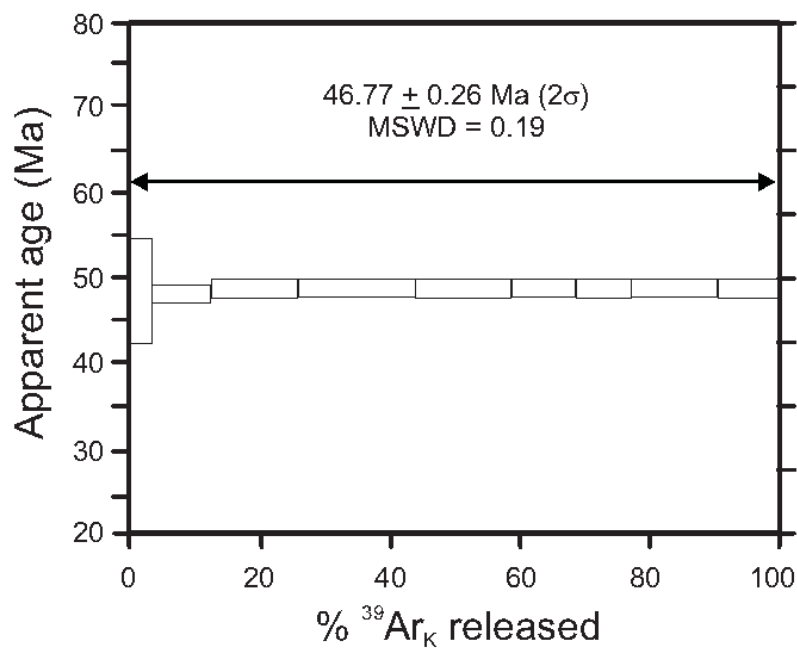


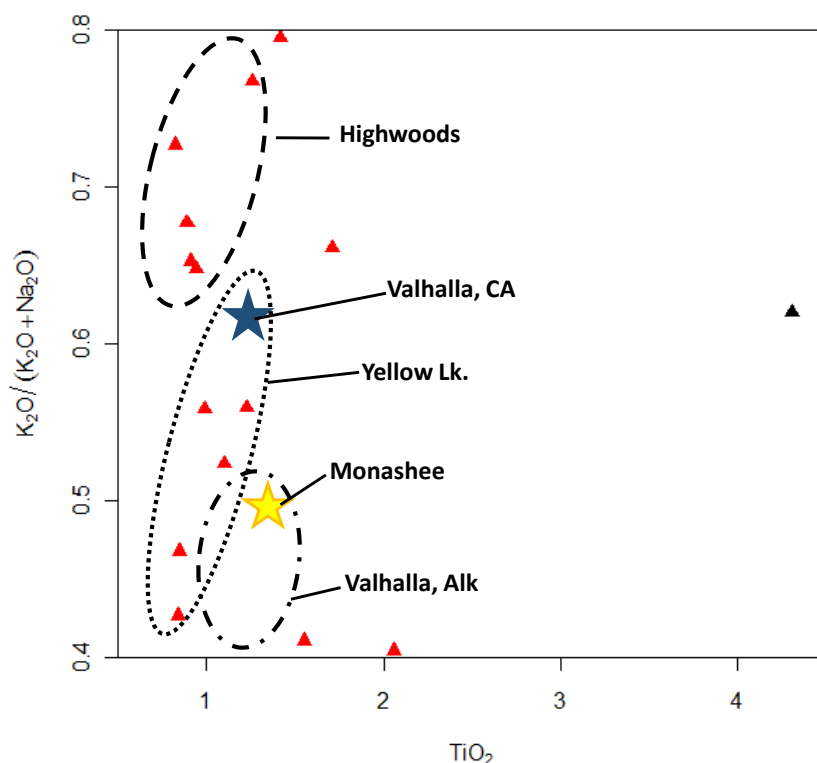Figure 8.  $^{40}Ar/^{39}Ar$ step-heating plot for lamprophyre sample LP17.

Figure 9.  $K_2O/(K_2O+Na_2O)$ vs. $TiO_2$ (wt.%) diagram (modified from Dostal and others, 2003, and O'Brien and others, 1995) comparing the lamprophyres of this study with selected mafic potassic rocks of southern British Columbia and the Highwood Mountains (Montana alkaline province). Red triangles are lamprophyres of this study; black triangle is Salmon River sample (LP17). Blue star is the average of Valhalla calc-alkaline lamprophyres (Sevigny, and others, 2003) and the yellow star is the average for Monashee calc-alkaline to shoshonitic lamprophyres (Adams, and others, 2005).

continental crust (and mantle lithosphere) to the east (Figure 1). Sample LP17 occurs immediately west of the arc-continent boundary and the 0.704/0.706 initial Sr isotope isopleth (Fleck and Criss, 2007; Blake and others, 2009). All the other samples intrude east of the continental 0.704/0.706 initial Sr isotope isopleth. Based on the limited data from this study, it appears the lithospheric mantle differs on either side of the 0.704/0.706 line.

Breitsprecher and others (2003) present geochemical contouring in their comparisons of lavas of the Eocene Challis-Kamloops volcanic belt to other Eocene volcanic occurrences in southern British Columbia and the Montana alkaline province. Specifically, they compared the ratios of $K_2O/SiO_2$, Rb/Zr, and Ta/Ce, to examine the alkalinity, relative enrichment, and tectonic

affinity of Eocene igneous rocks throughout this portion of the Pacific Northwest and southern British Columbia in the attempt to track the position of the Kula-Farallon slab window through Eocene time. The northern Idaho dikes reported in this study occur within their proposed Kula-Farallon slab window track of ca. 50 to 49 Ma. The lamprophyres of this study have $K_2O/SiO_2$ ratios ranging from 0.04 to 0.14, and Rb/Zr ratios ranging between 0.2 to 0.9, along with Ta/Ce ratios from 0.004 to 0.033. Although these values are not as elevated as either the Challis-Kamloops or Montana alkaline province rocks, they are higher than normal arc lavas. Detailed dating of the northern Idaho lamprophyre dikes could help resolve the age uncertainties as well as better understand the tectonic setting and thus allow testing of the Eocene Kula-Farallon slab window track model.

# SUMMARY

Fifteen post middle Eocene lamprophyre dikes were sampled in northern Idaho and northeastern Washington. Most of the dikes occur within the suprastructure (e.g., hanging wall) of the Priest River and Clearwater complexes, and none of the dikes show any metamorphic or deformational fabrics. The dikes are high-K to shoshonitic, calc-alkaline lamprophyres, and based on modal mineral assemblages, classify as kersantites, spessartites, and minettes. Geochemically, the lamprophyres have relatively high Mg#s (majority between 60 to 70) and exhibit LILE and LREE enrichments. Normalized trace element plots show distinctive negative anomalies in Nb, Ta, P, and Ti, characteristic of subduction-related melts. One lamprophyre dike occurs within the western Idaho shear zone along the main Salmon River, and is geochemically different than the remaining samples, with a less enriched character, lower Mg# (52), and no negative anomalies in Nb, Ta, P, and Ti. The Salmon River sample exhibits a $46.77 \pm 0.26$ Ma $^{40}Ar/^{39}Ar$ biotite date and is interpreted to having been generated from a different lithospheric mantle source than the lamprophyres to the north. The lamprophyres of this study have geochemical compositions comparable to other known Eocene-aged mafic potassic igneous rocks from British Columbia to the Highwood Mountains of the Montana alkaline province.

# ACKNOWLEDGMENTS

# REFERENCES CITED

Adams, M.G., Lentz, D.R., Shaw, C.S.F., Williams, P.F., Archibald, D.A., and Cousens, B., 2005, Eocene shoshonitic mafic dykes intruding the Monashee complex, British Columbia: a petrogenetic relationship with the Kamloops Group volcanic sequence?: Canadian Journal of Earth Sciences, v. 42, p. 11-24.

Blake, D.E., Gray, K.D., Giorgis, S., and Tikoff, B., 2009, A tectonic transect through the Salmon River suture zone along the Salmon River Canyon, in the Riggins region of west-central Idaho, *in* O'Connor, J.E., Dorsey, R.J., and Madin, I.P., eds., Volcanoes to Vineyards: Geologic Field Trips through the Dynamic Landscape of the Pacific Northwest: Geological Society of America Field Guide 15, p. 345-372.

Boynton, W.V., 1984, Cosmochemistry of the rare earth elements; meteorite studies, *in* Henderson, P., ed., Rare earth element geochemistry: Amsterdam, Elsevier Science Publishing. Co., p. 63-114.

Braudy, N., Gaschnig, R.M., Wilford, D., Vervoort, J.D., Nelson, C.L., Davidson, C., Kahn, M.J., and Tikoff, B., 2017, Timing and deformation conditions of the western Idaho shear zone, West Mountain, west-central Idaho: Lithosphere, v. 9, p. 157-183.

Breitsprecher, K., Thorkelson, D.J., Groome, W.G., and Dostal, J., 2003, Geochemical confirmation of the Kula-Farallon slab window beneath the Pacific Northwest in Eocene time: Geology, v. 31, no. 4, p. 351-354.

Cooper, A.F., 1979, Petrology of ocellar lamprophyres from western Otago, New Zealand: Journal of Petrology, v. 20, p. 139-163.

Dostal, J., Breitsprecher, K., Church, B.N., Thorkelson, D., and Hamilton, T.S., 2003, Eocene melting of Precambrian lithospheric mantle: Analcime-bearing volcanic rocks from the Challis-Kamloops belt of south central British Columbia: Journal of Volcanology and Geothermal Research, v. 126, p. 303-326.

Doughty, P.T., Chamberlain, K.R., Foster, D.A., and Sha, G., 2007, Structural, metamorphic, and geochronologic constraints on the origin of the Clearwater core complex, northern Idaho, *in* Sears, J.W., Harms, T.A., and Evenchick, C.A., eds., Whence the Mountains? Inquiries into the Evolution of Orogenic Systems: A Volume in Honor of Raymond A. Price: Geological Society of America Special Papers 433, p. 211-241.

Doughty, P.T., and Price, R.A., 1999, Tectonic evolution of the Priest River complex, northern Idaho and Washington: A reappraisal of the Newport fault with new insights on metamorphic core complex formation: Tectonics, v. 18, no. 3, p. 375-393.

Eby, G.N., 1980, Minor and trace element portioning between immiscible ocelli-matrix pairs from lamprophyre dykes and sills, Monteregian Hills petrographic province, Quebec: Contributions to Mineralogy and Petrology, v. 75, p. 269-278.

Fleck, R.J., and Criss, R.E., 2007, Location, age, and tectonic significance of the western Idaho suture zone, *in* Kuntz, M.A., and Snee, L.W., eds., Geological Studies of the Salmon River Suture Zone and Adjoining Areas, West-Central Idaho and Eastern Oregon: U.S. Geological Survey Professional Paper 1738, p. 15-50.

Giorgis, S., McClelland, W., Fayon, A., Singer, B., and Tikoff, B., 2008, Timing of deformation and exhumation in the western Idaho shear zone, McCall, Idaho: Geological Society of America Bulletin, v. 120, p. 1119-1133.

Harrison, T.M., Duncan, I., and McDougall, I., 1985, Diffusion of 40Ar in biotite: Temperature, pressure, and compositional effects: Geochimica et Cosmochimica Acta, v. 49, p. 2461-2468.

Hobbs, W., Griggs, A.B., Wallace, R.E., and Campbell, A.B., 1965, Geology of the Coeur d'Alene District, Shoshone County, Idaho: U.S. Geological Survey Professional Paper 478, 139 p.

Jicha, B.R., Scholl, D.W., Singer, B.S., Yogodzinski, G.M., and Kay, S.M., 2006. Revised age of Aleutian Island arc formation implies high rate of magma production: Geology, v. 34, p. 661-664.

Kuiper, K. F., Deino, A., Hilgen, F. J., Krijgsman, W., Renne, P. R., and Wijbrans, J. R., 2008, Synchronizing rock clocks of Earth history: Science, v. 320, no. 5875, p. 500-504.

Lewis, R., McFaddan, M., Burch, J., and McRaven Feeney, C., 2020, Idaho Rocks! A Guide to Geologic Sites in the Gem State: Missoula, Montana, Mountain Press, 160 p.

McDonough, W.F. and Sun, S.S., 1995, Composition of the Earth: Chemical Geology, v. 120, p. 223-253.

McDowell, F.W., 1971, K-Ar ages of igneous rocks from the western United States: Isochron/West, no. 2, p. 1-8.

Min, K., Mundil, R., Renne, P.R., and Ludwig, K.R., 2000, A test for systematic errors in $^{40}Ar/^{39}Ar$ geochronology through comparison with U/Pb analysis of a 1.1-Ga rhyolite: Geochimica et Cosmochimica Acta, v. 64, p. 73–98.

O'Brien, H. E., Irving, A.J., and McCallum, I.S., 1991, Eocene potassic magmatism in the Highwood Mountains, Montana: Petrology, geochemistry, and tectonic implications: Journal of Geophysical Research, v. 96, no. B8, p. 13,237-13,260.

O'Brien, H. E., Irving, A.J., and McCallum, I.S., and Thirwall, M.F., 1995, Strontium, neodymium and lead isotopic evidence for interaction of post-subduction asthenospheric potassic mafic magmas of the Highwood Mountains, Montana, USA, with ancient Wyoming craton lithospheric mantle: Geochimica et Cosmochimica Acta, v. 59, p. 4539-4556.

Peccerillo, A., and Taylor, S.R., 1976, Geochemistry of Eocene calc-alkaline volcanic rocks from the Kastamonu area, Northern Turkey: Contributions to Mineralogy and Petrology, v. 58, p. 63-81.

Philpotts, A.R., 1976, Silicate liquid immiscibility: its probable extent and petrogenetic significance: American Journal of Science, v. 276, p. 1147-1177.

Rock, N.M.S., 1984, Nature and origin of calc-alkaline lamprophyres: minettes, vogesites, kersantites and spessartites: Earth and Environmental Science Transactions of the Royal Society of Edinburgh, v. 74, p. 193-227.

Rock, N.M.S., 1987, The nature and origin of lamprophyres: an overview, *in* Fitton, J.G. and Upton, B.G.J. eds., Alkaline igneous rocks:

Geological Society of London, Special Publication 30, p. 191-226.

Rock, N.M.S., Bowes, D.R., and Wright, A.E., 1991, Lamprophyres: Blackie, Glasgow and London, 285 p.

Schmidt, K.L., Gray, K.D., Lewis, R.S., Steven, C., and Isakson, V.H., 2016, Mesozoic tectonics west of the accretionary boundary in west-central Idaho: A road log along U.S. Highway 95 between Moscow and New Meadows, Idaho, *in* Lewis, R.S, and Schmidt, K.L., eds., Exploring the Geology of the Inland Northwest: Geological Society of America Field Guide 41, p. 175-209.

Sevigny, J.H. and Theriault, R.J., 2003, Geochemistry and Sr-Nd isotopic composition of Eocene lamprophyre dykes, southeastern British Columbia: Canadian Journal of Earth Sciences, v. 40, p. 853-864.

Shannon, E.V., 1920, Petrography of some lamprophyric dike rocks of the Coeur d'Alene mining district, Idaho: U.S. National Museum Proceedings, v. 57, p. 475-495.

Winter, J.D., 2001, An Introduction to Igneous and Metamorphic Petrology: Upper Saddle River, New Jersey, Prentice Hall Inc., 697 p.

Woolley, A.R., Bergman, S.C., Edgar, A.D., LeBas, M.J., Mitchell, R.H., Rock, N.M.S., and Scott Smith, B.H., 1996, Classification of lamprophyres, lamproites, kimberlites, and the kalsilitic, melilitic, and leucitic rocks: The Canadian Mineralogist, v. 34, p. 175-186.

# APPENDIX 1:
# lamprophyre sample locations, type, and geologic setting

| Sample number | Rock Type | Latitude | Longitude | Geologic Setting |
|---|---|---|---|---|
| 01LP16 | spessartite | 47.5799 | -116.2541 | CDA Dist., Belt SG |
| 02LP16A | kersantite | 47.4347 | -116.3514 | CDA Dist., Belt SG |
| 02LP16B | spessartite | 47.4347 | -116.3514 | CDA Dist. Belt SG |
| 03LP16 | kersantite | 48.3961 | -116.3874 | in granitic, east PRC |
| 04LP16 | minette | 48.1799 | -116.4288 | Belt SG, east PRC |
| 05LP16 | minette | 48.1771 | -116.4166 | Belt SG, east PRC |
| 06LP16 | kersantite | 48.9759 | -117.3118 | in Metaline Fm. |
| 07LP16 | spessartite | 48.4923 | -116.4016 | Belt SG, east PRC |
| 09LP16 | kersantite | 48.5059 | -116.4067 | Belt SG, east PRC |
| 11LP16 | kersantite | 48.5101 | -116.3980 | Belt SG, east PRC |
| 14LP16 | minette | 48.2553 | -116.4413 | Belt SG, east PRC |
| 15LP16 | spessartite | 46.8943 | -116.2591 | Clearwater complex |
| 16LP16 | spessartite | 46.9101 | -116.2671 | Clearwater complex |
| 17LP16 | spessartite | 45.4186 | -116.1721 | western ID shear zone |
| 18LP16 | kersantite | 48.0958 | -117.3186 | in granitic, west PRC |

# APPENDIX 2:
## $^{40}$Ar/$^{39}$Ar biotite age of lamprophyre dike

A lamprophyre dike (LP17) was collected along the main Salmon River of west-central Idaho. The sample was crushed, sieved, and several large biotite crystals (1-2 mm diameter) were picked. The biotite was loaded into an aluminum disk, along with the 28.201 Ma Fish Canyon sanidine standard (Kuiper and others, 2008), and irradiated at the Oregon State University TRIGA reactor. Corrections for undesirable nucleogenic reactions are as follows: $(^{40}Ar/^{39}Ar)_K$ = 0.00086; $(^{38}Ar/^{39}Ar)_K$ = 0.01211; $(^{36}Ar/^{37}Ar)_{Ca}$ = 0.000264; and $(^{39}Ar/^{37}Ar)_{Ca}$ = 0.000673. The decay constants of Min and others (2000) were used in the age calculations.

Following irradiation, a single crystal of biotite was incrementally heated using a 25W $CO_2$ laser at the University of Wisconsin Rare Gas Geochronology Laboratory. Gas cleanup followed the procedures outlined in Jicha and others (2006). Blanks were measured after every two heating steps. The isotopic composition of the gas was measured with a Mass Analyzer Products-215-50 mass spectrometer.

The biotite yielded a plateau age of 46.77 ± 0.26 Ma (2σ analytical uncertainty + J uncertainty). $^{40}$Ar/$^{39}$Ar biotite ages should record closure temperatures of 300°C - 350°C (Harrison and others, 1985). Given that apatite fission track age – indicating closure through ~120°C – at 40-50 Ma (Giorgis and others, 2008) in the rock sample from the WISZ (LP17), we assume that the region around the ~ 2 m wide dike was relatively cool prior to emplacement. As a result, we anticipate relatively rapid cooling, and that the $^{40}$Ar/$^{39}$Ar biotite age locked in shortly (< 0.1 m.y.) after dike emplacement.